Lasers in Manufacturing Conference 2025

Powder channel roughness effects on particle flow and nozzle durability in laser-based directed energy deposition

Annika Bohlen[a,*], Thomas Seefeld[a,b]

[a]*BIAS – Bremer Institut für angewandte Strahltechnik GmbH, Klagenfurter Straße 5, 28359 Bremen, Germany*
[b]*MAPEX Center for Materials and Processes – University of Bremen, Bibliothekstraße 1, 28359 Bremen, Germany*

Abstract

In laser-based directed energy deposition (DED), a well-aligned powder stream relative to the laser beam is essential for maximizing process efficiency and minimizing material loss. A detailed understanding of powder stream propagation is therefore critical. In this study, high-speed imaging was used to investigate particle behavior within the powder stream. Using a multi-step evaluation method, the mean velocity, velocity variations, and flight direction of individual particles were determined. Powder channels with varying surface roughness—ranging from Ra = 2.16 µm to 0.27 µm—were tested to assess their influence on stream characteristics. The results reveal that lower channel roughness leads to increased mean particle velocity and significantly narrower flight angles. Specifically, the divergence angle decreased by approximately 61 %, which suggests the potential for a more focused powder stream and reduced material loss. In addition to these findings, 70-hour endurance tests confirmed the long-term stability of particle flow and divergence, with no measurable changes observed. Surface topography evolved slightly due to particle impact, but roughness values remained stable and no structural degradation occurred. These findings offer valuable insights into optimizing powder delivery systems for enhanced efficiency and precision in laser-based DED processes.

Keywords: Laser-based Directed Energy Deposition, Powder Nozzle, Powder Stream Propagation

1. Introduction

Over the past few decades, laser-based directed energy deposition (DED) has emerged as a key technology, not only for additive manufacturing of components but also for the refurbishment of high-value parts (Schmidt et al. 2017). Achieving cost-effective operation requires optimization of both process and material efficiency. The powder delivery system plays a central role in both. From a resource efficiency standpoint, maximizing powder utilization is critical—minimizing material loss while simultaneously supporting high deposition rates. A greater stand-off helps shield the nozzle from thermal exposure and prevents accumulation of particles on its surface. A wide processing range, on the other hand, helps maintain stable deposition even if minor variations occur in nozzle-to-substrate distance. Maintaining a narrow powder stream with minimal divergence is key to achieving both a large stand-off and precise material delivery. Meeting these design requirements is essential for ensuring robust component manufacturing and repair.

In addition to the commonly used powder nozzle configurations, a number of alternative concepts have been developed for specialized applications. One widely used design is the internal coating nozzle. Other nozzle concepts focus on improved shielding gas coverage for the processing of highly reactive materials (Cortina et al. 2018; Ruiz et al. 2022), or on achieving particularly high build-up rates (Kim et al. 2021). Most powder nozzles are manufactured from copper-based alloys due to their favorable thermal conductivity and good machinability. However, these materials tend to exhibit limited wear resistance. As a result, the geometry and quality of the powder stream can change over the course of the nozzle's service life. (Tan et al. 2020) observed a significant deterioration in powder stream convergence during experimental studies on a

*Corresponding author. Tel.: +49 421 218 58110.
E-mail address: bohlen@bias.de.

single-injector copper nozzle subjected to prolonged use. After 60 hours of powder feeding, the powder spot diameter at a plane 15 mm below the nozzle exit increased by 41.4 %. This degradation was attributed to erosive wear at the nozzle tip, which also caused a reduction in the deposited layer height over time. The interaction between the laser beam, melt pool, and powder stream was consequently impaired, leading to reduced process stability and geometrical inconsistencies.

For applications that require customized nozzle geometries or small production volumes—such as designs with integrated cooling channels—powder nozzles can be manufactured using laser powder bed fusion (PBF-LB) (Bernhard et al. 2020). However, there is limited understanding of how the internal powder channels of such additively manufactured nozzles must be processed to ensure high-quality and consistent powder stream characteristics. Furthermore, the durability and long-term performance of these novel designs remain largely unknown.

The aim of this work is to systematically investigate the powder stream characteristics and durability of such additively manufactured nozzles from high-hardness copper alloy. Particular focus is placed on examining how the internal surface roughness of the powder channels affects particle trajectories and the divergence angle of the powder stream. In addition, the long-term stability of these nozzles under continuous powder feeding conditions is evaluated to assess the suitability of the selected material and the consistency of performance over extended operation.

2. Experimental Setup and Methods

2.1. Materials

The powder material used in this study was a nickel-based alloy (EuTroloy 16625G.04) provided by Castolin Eutectic Ireland Ltd. Scanning electron microscopy (SEM) images (Fig. 1a) reveal that the powder consists predominantly of spherical particles, including some with satellite structures. A minority of particles display irregular morphologies. In Fig. 1b the particle size distribution is shown, with D10, D50, and D90 values of 65 µm, 99 µm, and 138 µm, respectively. The powder was conveyed through the nozzle using a disk feeder supplied by BLC.

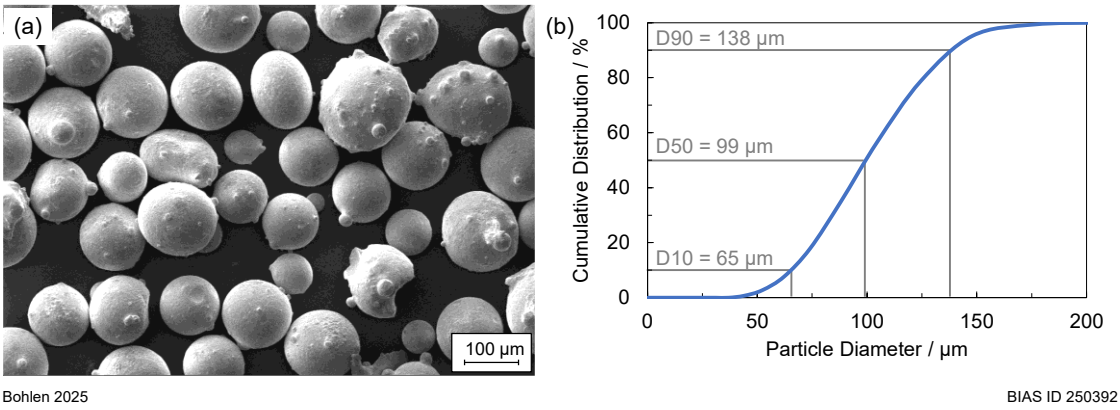

Fig. 1. (a) SEM image of the powder (b) powder size distribution

As the nozzle body, cuboids made from HOVADUR CNCS (a thermally age-hardenable copper-nickel-silicon alloy with added chromium) were manufactured via laser powder bed fusion by Schmelzmetall (see Fig. 2a). The composition of HOVADUR CNCS is given in Table 1. According to the manufacturer's data sheet, the material exhibits high electrical and thermal conductivity combined with high hardness and mechanical strength, as well as good corrosion and wear resistance. In the hardened condition, the Brinell hardness is specified to be at least 190 HB, and the average thermal conductivity in the temperature range of 20°C to 300 °C is approximately 220 W/m·K. After fabrication, the specimens underwent a heat treatment process to optimize their microstructural and mechanical properties. Metallographic analysis revealed a homogeneous microstructure without any detectable cracks and with very low porosity (Fig. 2 (b)). Hardness measurements were carried out at five different locations on each specimen, yielding an average value of 239 HBW 1/10 ± 3 HBW 1/10. Powder channels were subsequently introduced into these cuboids using wire electrical discharge machining (EDM), carried out by Institute for Machine Tools and Factory Management, Technische Universität Berlin. Five channels were produced, each with different levels of internal surface roughness. The channels had a circular cross-section with a diameter of 1.54 mm ± 0.04 mm and an effective length of 19 mm after thread insertion.

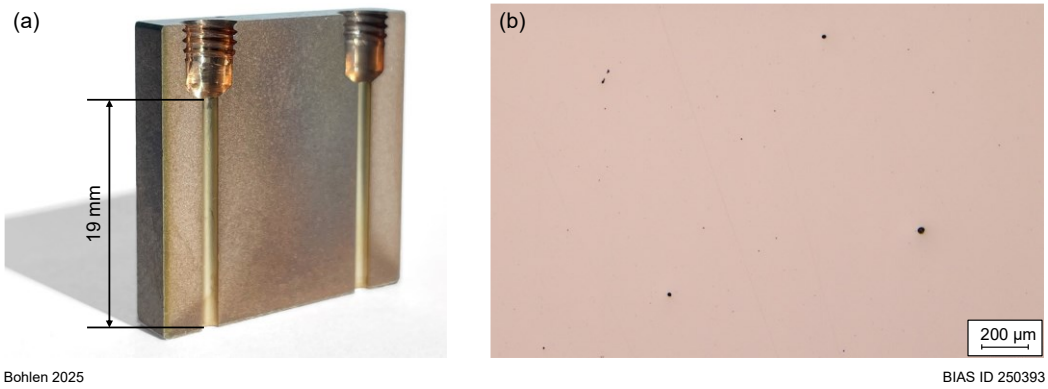

Fig. 2. (a) HOVADUR CNCS specimen manufactured by powder bed fusion, with integrated powder channels created via wire EDM; the sample was sectioned in half using EDM for characterization (b) Macroscopic cross-sectional view of the specimen

Table 1. Chemical composition in % of weight of HOVADUR CNCS

Ni	Si	Cr	Fe	Mn	Pb	Other metals	Cu
2.0% - 3.0%	0.5% - 0.8%	0.2% - 0.5%	max. 0.15%	max. 0.1%	max. 0.02%	max. 0.1%	Bal.

To allow for surface roughness characterization, the channels were sectioned using EDM. A Keyence VK 9700 confocal laser scanning microscope was used for this purpose, operating at 50× magnification. Prior to roughness analysis, the surface topography was corrected to remove curvature artifacts. The data were then filtered using a short-wavelength cutoff (λs) of 0.8 µm and a long-wavelength cutoff (λc) of 0.8 mm (see topography in Fig. 3a). For the line-based surface roughness analysis, ten parallel profiles were extracted at intervals of 14 µm. From these profiles, the arithmetical mean roughness (Ra) was calculated. A summary of all measured values is presented in Fig. 3b.

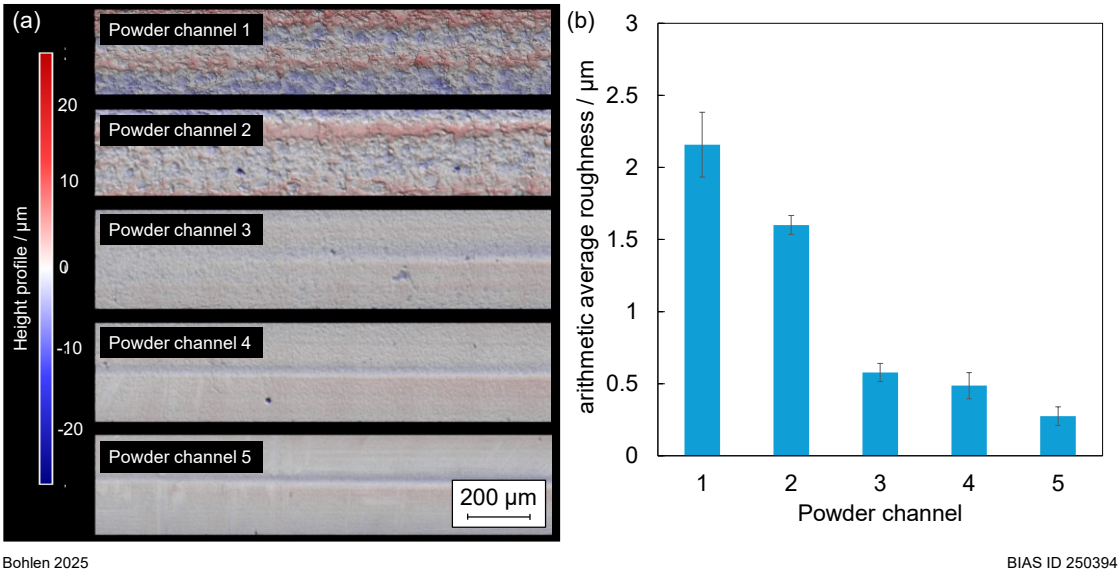

Fig. 3. (a) Topography of the powder channels (b) Measured values of the arithmetical mean surface roughness (Ra) for each of the five powder channels.

2.2. High-speed imaging and analysis

High-speed imaging of the particle-laden stream was carried out using an i-Speed 7 camera (iX Cameras), operating at 45 kHz. Illumination was provided by a Cavilux laser system (Cavitar), which ensured sufficient contrast for automated particle detection following background subtraction. Particle detection and trajectory reconstruction were performed using the TrackMate plugin (Ershov et al. 2022) in ImageJ.

Each particle's path was analyzed to determine its mean velocity and angle of flight, see Fig. 4. Tracks indicating negative velocities (i.e., rebounding particles) were excluded. Distributions of particle velocities and their corresponding angles were analyzed using binned statistics based on the Freedman–Diaconis rule. For each velocity bin, the standard deviation (2σ) of the particle angles was calculated to assess the angular spread.

To evaluate the powder stream divergence, the binary images were integrated to yield a cumulative intensity map. From this, a line profile was extracted perpendicular to the jet direction, located 10 mm downstream of the nozzle exit. A Gaussian fit was applied to this profile, with the standard deviation of the intensity defining the boundaries of the powder stream. The divergence angle was calculated between the boundaries (Bohlen and Seefeld 2024a).

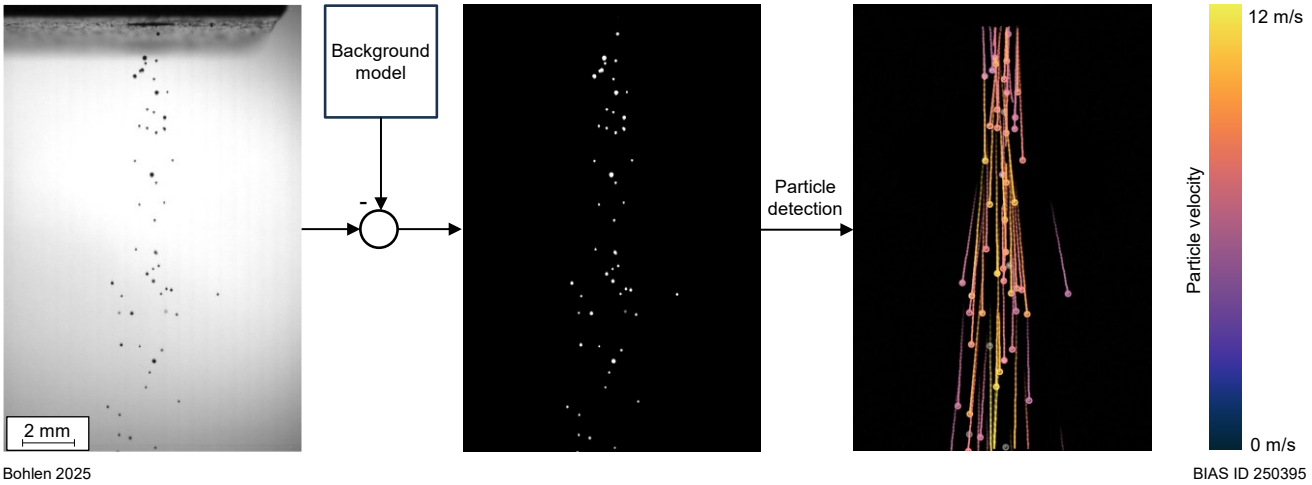

Fig. 4. Evaluation procedure of the high-speed videos

For durability testing, the powder injector was operated in 10-hour intervals, with powder being fed continuously and collected after each interval. The collected powder was sieved and reused in subsequent intervals to simulate long-term use. In total, the nozzle was tested for 70 hours. After each 10-hour segment, high-speed recordings of the powder stream were taken to evaluate the particle velocity and divergence angle, using the same methodology as previously described. Air was used as the carrier gas, passed through an oil removal system to ensure cleanliness. The carrier gas flow rate was maintained at 3.5 l/min, and the powder feed rate was set to 10 g/min. For these measurements, a Photron Nova S12 high-speed camera operating at 40 kHz was employed.

3. Results

Fig. 5a presents particle velocity as a function of carrier gas flow rate for all tested channel roughnesses. A near-linear rise in particle velocity is observed with increasing gas flow across all channels. The roughest channel results in the lowest particle velocities, while the second smoothest channel consistently achieves the highest particle velocities at all gas flow rates.

Fig. 5b illustrates the relationship between particle velocity and increasing powder mass flow rate for various internal channel roughness levels. The results show that particle velocity remains largely unaffected by changes in powder mass flow rate. Similar to the carrier gas flow rate trend, the channel with the highest roughness (Ra) consistently yields the lowest particle velocities, whereas the second smoothest channel produces the highest particle velocities.

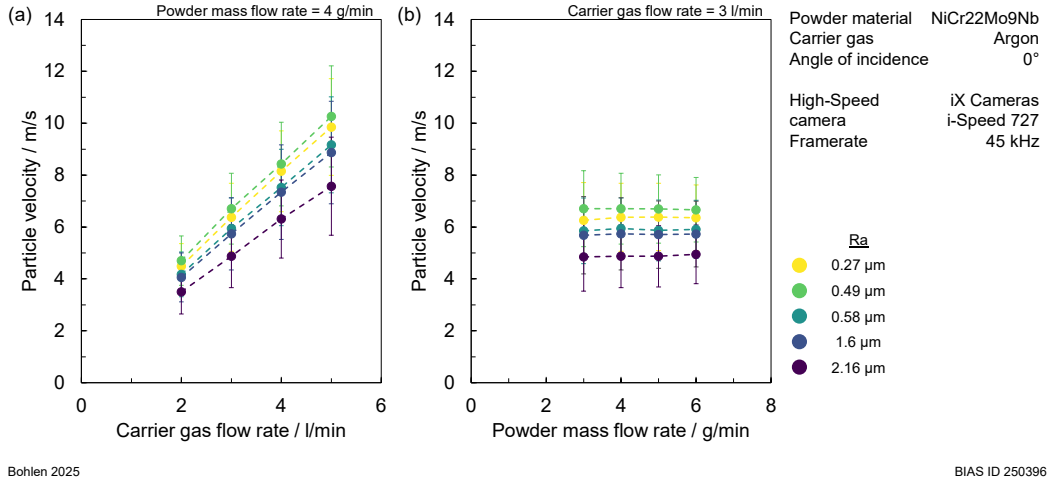

Fig. 5. Particle velocity as a function of (a) the carrier gas flow rate and (b) the powder mass flow rate for different inner channel roughness Ra

Fig. 6a illustrates how the divergence angle of the powder stream changes with varying carrier gas flow rates across different internal channel roughness levels. Across all surface conditions, a slight increase in divergence angle is observed as the carrier gas flow increases. As expected, the smoothest channel (Ra = 0.27 µm) consistently produces the narrowest divergence angles, while the roughest surface results in the widest spread of the powder stream.

Fig. 6b presents the divergence angle as a function of powder mass flow rate for the same set of surface finishes. For the two roughest channels, a reduction in divergence angle is seen with increasing powder flow. In contrast, the three smoother channels exhibit relatively constant divergence angles regardless of powder mass flow rate. Overall, the divergence angle increases with increasing surface roughness.

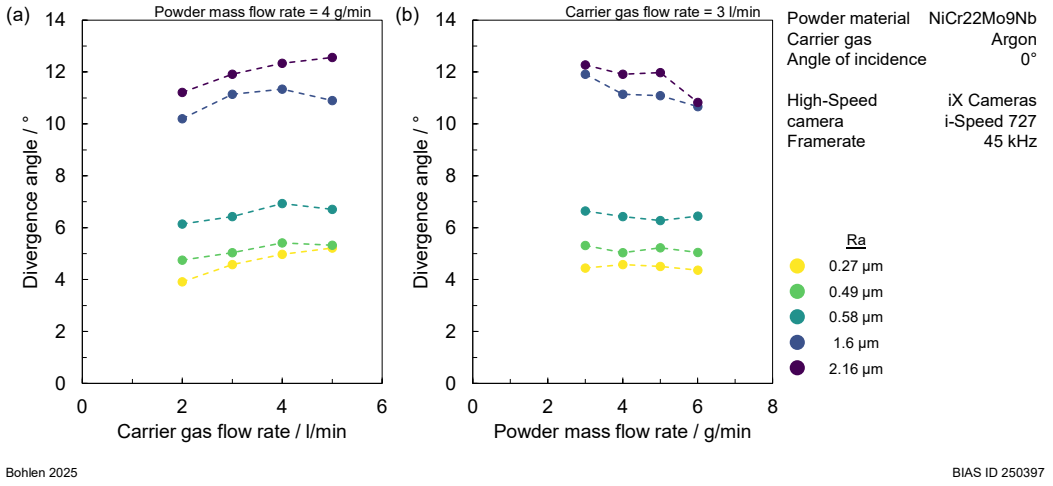

Fig. 6. Divergence angle as a function of (a) the carrier gas flow rate and (b) the powder mass flow rate for different inner channel roughness Ra

Fig. 7a displays a scatter plot illustrating individual particle velocities alongside their corresponding flight angles, based on a 222.2 ms segment of high-speed video analysis. Each data point represents a single tracked particle. The distribution of flight angles is centered symmetrically around 0°, with the broadest flight angle occurring at lower particle velocities, around 2 m/s. As particle velocity increases, the angular deviation narrows, converging toward 0°. The maximum recorded particle velocities reach approximately 7 m/s. Fig. 7b shows a comparable measurement using a powder channel with reduced surface roughness (Ra = 0.27 µm). In this case, the angular spread is notably narrower, while the maximum particle velocities remain similar to those observed in Fig. 7a. Fig. 7c and d depict the same measurements under increased carrier gas flow conditions (5 l/min) for both roughness levels. Although the maximum flight angles remain comparable to those at lower gas flow rates, the particle velocity distributions shift toward higher values. For the higher-roughness channel, velocities range from 5 m/s to 12 m/s, while for the smoother channel, they extend from 6 m/s to 15 m/s. In all cases, the angular distribution remains symmetric about 0°, further highlighting the directional consistency of the powder stream.

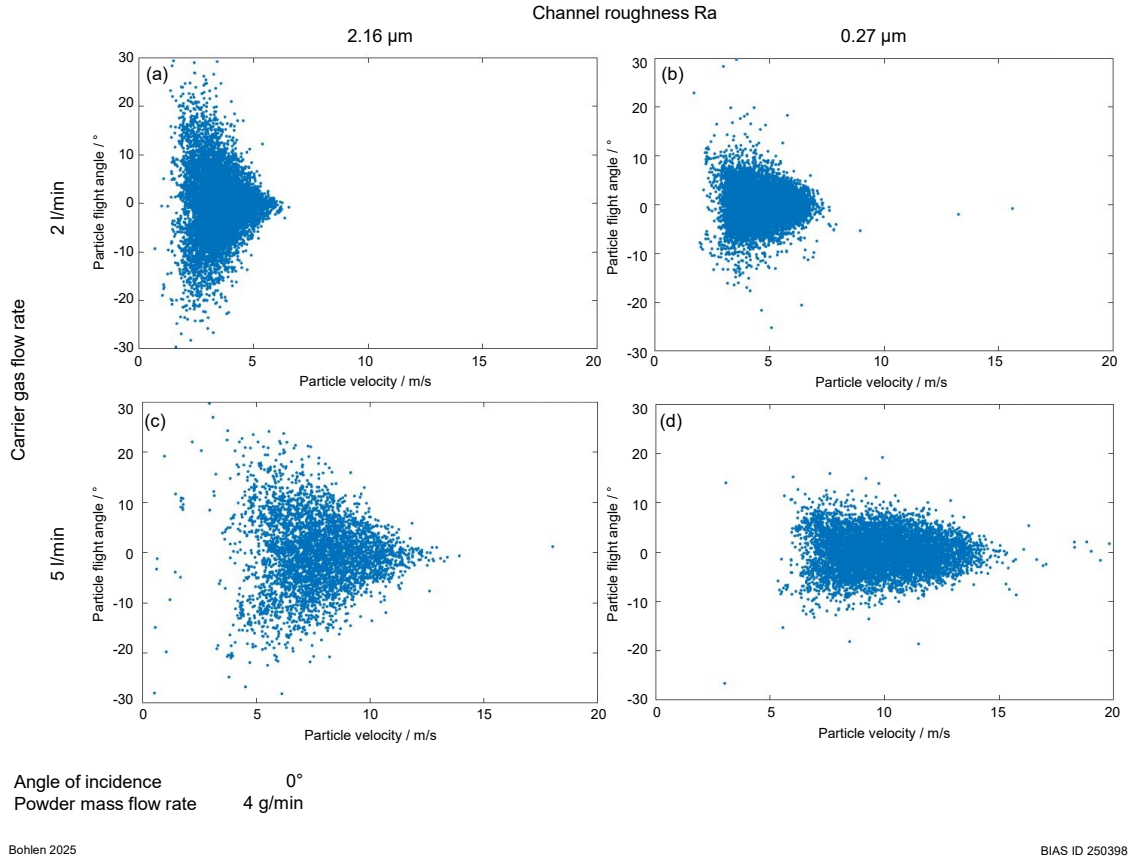

Fig. 7. Flight angles and corresponding particle velocities of tracked particles for (a) the high-roughness channel (Ra = 2.16 µm) under low carrier gas flow conditions (2 l/min) (b) low-roughness channel (Ra = 0.27 µm) with a low carrier gas flow rate (2 l/min) (c) high-roughness channel (Ra = 2.16 µm) with a low carrier gas flow rate (2 l/min) (d) low-roughness channel (Ra = 0.27 µm) with a high carrier gas flow rate (5 l/min)

To support direct comparison between all conditions, Fig. 9 presents only the two-sigma bounds of the particle flight angle distributions. The analysis shows that particle flight angle decreases with increasing particle velocity. Across all tested powder channel roughness levels, the maximum particle velocity is comparable and reaches approximately 9 m/s. However, differences become apparent in the distribution of slower particles. In channels with low surface roughness, slow-moving particles typically travel at around 4 m/s with flight angles near 15°. In contrast, rougher powder channels produce particles that travel as slowly as 3 m/s and exhibit flight angles of up to 25°.

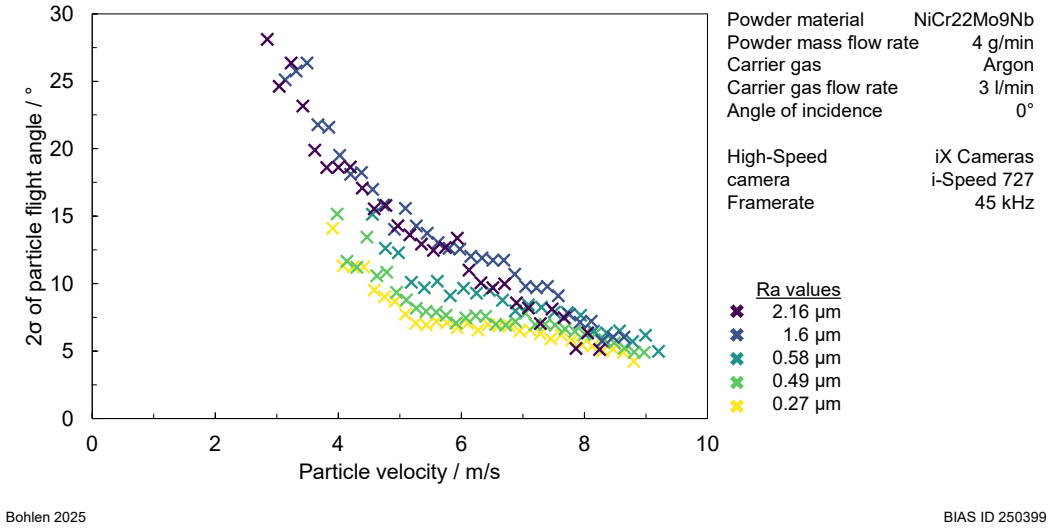

Fig. 9. Two sigma standard deviation of the particle flight angle as a function of the particle velocity for different Ra values

The endurance tests focused on the smoothest powder channel. Fig. 8a illustrates the particle velocity as a function of powder feed time over a total duration of 70 hours. The data show a stable behavior with an average particle velocity of approximately 4.8 m/s. Notably, the standard deviation of the particle velocity remains constant throughout the entire testing period, indicating consistent flow conditions. Fig. 8b presents the evolution of the powder stream's divergence angle over time. Similar to the particle velocity, no significant changes are observed. The divergence angle remains stable at around 3.5°.sss

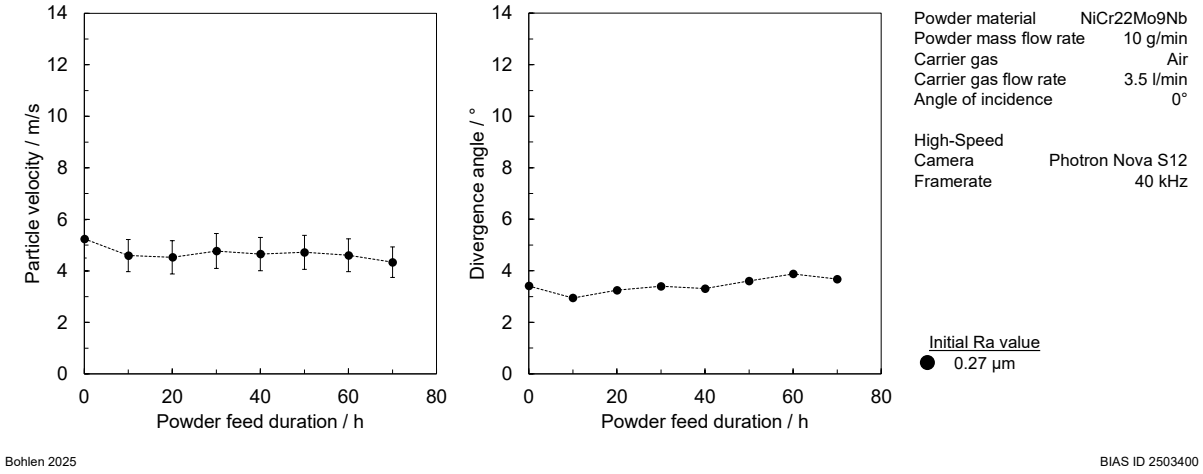

Fig. 8. (a) Particle velocity and (b) divergence angle as a function of the powder feed duration for smoothest channel roughness

Fig. 10 presents the results of surface roughness analysis before and after endurance testing. The powder channels roughness Ra remains largely unchanged over time, while the internal surface topography exhibited noticeable alterations. The measured surface roughness before endurance testing is reported as Ra = 0.27 µm. The image Fig. 10a) shows a relatively smooth surface with some visible horizontal and vertical features. The reported surface roughness after endurance testing is Ra = 0.23 µm. The surface appears more homogeneous and exhibits a wave-like texture, see Fig. 10b. Fig. 10c shows the material ratio curves for the two surfaces. The blue curve (0 h) drops more sharply at the beginning, indicating that a larger portion of the surface height lies at the uppermost peaks. The magenta curve (70 h) descends more gradually and smoothly, indicating that the surface has a more uniform height distribution. Toward the lower material ratios (i.e., deeper into the surface), the magenta curve stays slightly above the blue.

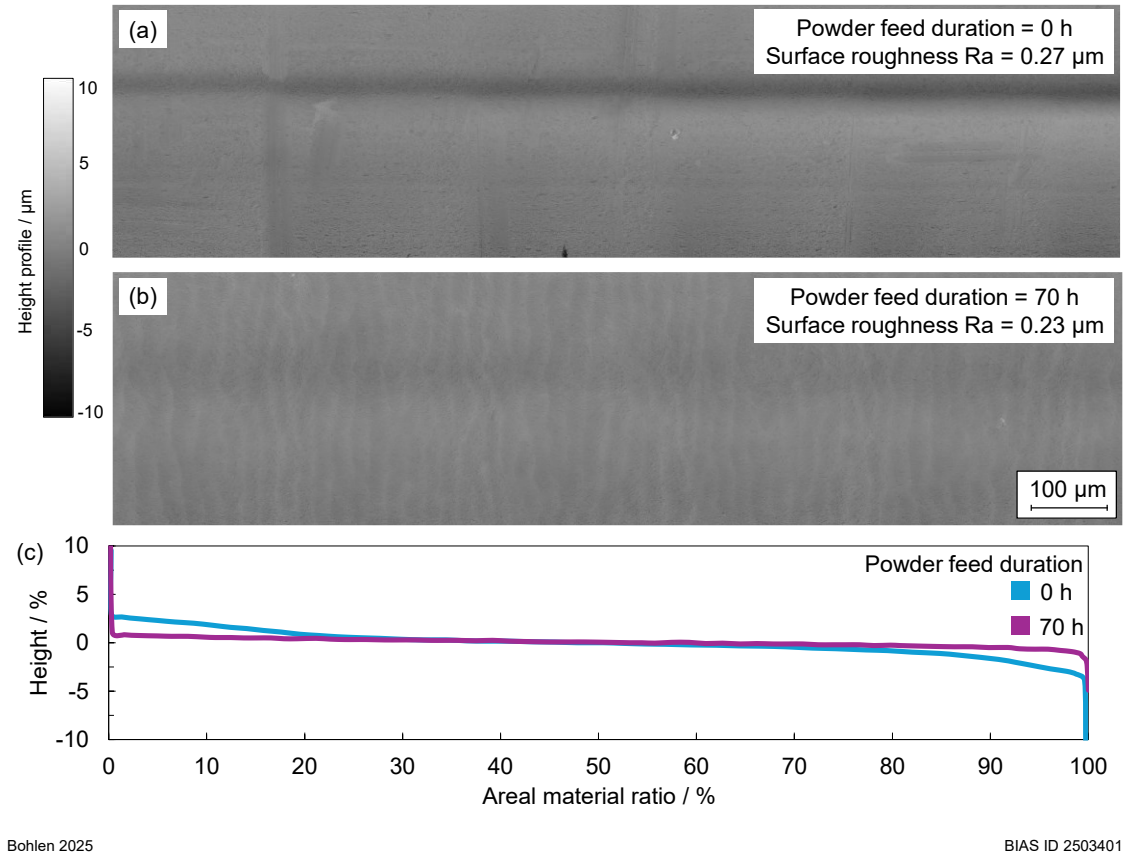

Fig. 10. Surface topography of the smoothest powder channel (a) before endurance testing and (b) after 70 hours of endurance testing and (c) the material ratio curve for both surfaces

4. Discussion

The results indicate that particle velocity is influenced by several parameters, with carrier gas flow rate showing a nearly linear relationship to particle velocity (Fig. 5a). With a constant internal diameter of the powder channel, increasing the carrier gas flow rate leads directly to a higher gas velocity, which in turn enhances the acceleration of particles. Thus, carrier gas dynamics play a dominant role in determining particle speed. Aside from gas flow rate, the internal surface condition of the powder channel also affects particle velocity. Smoother surfaces tend to promote slightly higher particle velocities (Fig. 5a). This can be explained by the reduction of particle-wall interactions in smoother channels. When a particle collides with the inner wall of the injector, it is decelerated upon impact and its direction of motion is altered. According to (Sommerfeld 1992; Sommerfeld and Huber 1999), the angle by which a particle deviates from the wall-normal following a collision can be described using a statistical distribution. The spread of this deviation—often referred to as the standard deviation of the reflection angle—increases with surface roughness (Ra). In other words, rougher channel walls lead to a broader distribution of rebound angles, meaning that particles are more likely to be scattered after each impact. As a result, particles traveling through rougher channels are statistically more likely to experience multiple wall collisions throughout

their trajectory. Each additional collision leads to further energy loss and direction change, reducing the overall efficiency of acceleration by the carrier gas. This cumulative effect explains why smoother channels enable higher mean particle velocities, as particles maintain more linear paths and encounter fewer energy-dissipating interactions (Bohlen and Seefeld 2024b). In contrast, powder mass flow rate does not have a significant impact on particle velocity (Fig. 5b). Given the relatively low powder loading in the gas stream during the experiments, particle-particle interactions are minimal, and therefore, changes in mass flow do not significantly affect momentum transfer within the stream.

The divergence angle of the powder stream is found to be primarily influenced by the surface roughness inside the powder channel. As roughness increases, the divergence angle also increases (Fig. 6a), regardless of carrier gas flow rate. This confirms that divergence is largely independent of carrier gas flow and primarily governed by surface-driven scattering mechanisms. The angular deviation of particle trajectories at the channel exit appears to result from the final particle-wall collision inside the channel. In smoother channels, particles tend to follow straighter, more focused paths, while rougher surfaces cause more deflection, increasing the angular spread. This interpretation is reinforced by the scatter plots in Fig. 7. Particles traveling at higher velocities are generally associated with smaller flight angles, suggesting they were not deflected just before exiting the channel. Conversely, larger flight angles are likely the result of late-stage collisions near the nozzle exit, which prevent further acceleration and result in wider powder stream divergence. Fig. 9 further supports this by showing that smoother channels produce a narrower distribution of particle flight angles, emphasizing the role of internal wall conditions in directing particle trajectories.

Over the 70-hour test period, no significant changes in particle velocity or divergence angle were observed (Fig. 8). This consistent performance suggests that the nozzle material is well-suited for sustained industrial use, particularly when compared to findings reported by (Tan et al. 2020), who observed functional changes in related systems over time. The durability of the nozzle can be attributed to the use of a high-hardness copper alloy, which maintained a smooth surface even after prolonged exposure to abrasive particle flow. Although surface topography changes were observed post-testing—due to continuous particle impacts—no structural damage or surface degradation was identified, see Fig. 10. The surface showed signs of mild texture evolution, resembling controlled surface conditioning or matting, similar in appearance to the effects of fine abrasive blasting. The impacts altered only the microtexture without significantly affecting the macroscopic surface profile. This is further supported by the material ratio curves shown in Fig. 10c. The curve for the unused surface (blue, 0 h) drops steeply, indicating a greater concentration of elevated surface features. In contrast, the curve after 70 hours of powder exposure (magenta) declines more gradually, suggesting a more uniform height distribution. The slightly higher profile of the magenta curve in the lower material ratio region confirms that the surface evolved toward a smoother and more evenly distributed topography.

5. Conclusion

This study investigated the influence of internal powder channel surface roughness on the behavior of particle-laden flow in laser-based directed energy deposition nozzles. Using laser powder bed fusion–fabricated high-hardness copper alloy specimens, five channels with varying surface roughness were analyzed to assess their effects on particle velocity, powder stream divergence, and long-term durability. High-speed imaging and trajectory tracking were employed to evaluate particle behavior, while endurance testing over 70 hours was conducted to examine wear effects and flow stability.

- Powder stream divergence is strongly influenced by the internal surface roughness, with smoother powder channels consistently producing a narrower and more focused powder jet.
- A reduction in surface roughness (Ra) from 2.16 µm to 0.27 µm resulted in a 61 % decrease in the mean divergence angle, emphasizing the critical role of surface finish in maintaining jet stability and directionality.
- While the carrier gas flow rate significantly affects particle velocity, it has no observable influence on the divergence angle, which is primarily determined by the surface condition of the powder channel.
- Endurance tests conducted over 70 hours revealed no measurable change in either particle velocity or divergence angle, indicating stable and consistent nozzle performance during prolonged operation.
- Although the internal surface topography changed slightly due to continuous particle impact, the Ra values remained constant, suggesting that the surface underwent mild, non-destructive texturing without erosion or damage.
- Laser powder-bed fusion has proven to be a suitable method for manufacturing customized powder nozzles, provided that careful post-processing of the internal channels is carried out to achieve optimal flow characteristics.

Acknowledgements

The authors gratefully acknowledge the collaboration with the project partners Nutech GmbH, Schmelzmetall Deutschland GmbH and Technische Universität Berlin regarding the support of knowledge, material and equipment over the course of the research.

The ZIM-project No. KK5274710EW2 was funded by the Federal Ministry for Economic Affairs and Climate Action (BMWK) via the German Federation of Industrial Research Associations (AiF) in accordance with the policy to support the Central Innovations of Medium-Sized Enterprises (ZIM) based on a decision by the German Bundestag.

LUNOVU 835 LMD-Machine is funded by the Deutsche Forschungsgemeinschaft (DFG, German Research Foundation) – project number 434424600 (Highly flexible material synthesis and microstructure adjustment through combined laser deposition welding and short-term heat treatment for high-throughput materials development).

References

Bernhard, R., Neef, P., Eismann, T., Wiche, H., Hoff, C., Hermsdorf, J. et al., 2020. Additive manufacturing of LMD nozzles for multi-material processing. Procedia CIRP 94, pp. 336–340.

Bohlen, A., Seefeld, T., 2024a. Adaptive powder nozzle setup for enhanced efficiency in laser metal deposition. Journal of Laser Applications 36 (1), Article 012017.

Bohlen, A., Seefeld, T., 2024b. Influence of the inner roughness of powder channels on the powder propagation behavior in laser metal deposition. Journal of Laser Applications 36 (4), Article 042007.

Cortina, M., Arrizubieta, J. I., Ruiz, J. E., Lamikiz, A., Ukar, E., 2018. Design and Manufacturing of a Protective Nozzle for Highly Reactive Materials Processing via Laser Material Deposition. Procedia CIRP 68, pp. 387–392.

Ershov, D., Phan, M.-S., Pylvänäinen, J. W., Rigaud, S. U., Le Blanc, L., Charles-Orszag, A. et al., 2022. TrackMate 7: integrating state-of-the-art segmentation algorithms into tracking pipelines. Nature methods 19 (7), pp. 829–832.

Kim, C. K., Jeong, J. I., Choi, S. G., Kim, J. H., Cho, Y. T., 2021. High-throughput directed energy deposition process with an optimized scanning nozzle. Journal of Materials Processing Technology 295, p. 117165.

Ruiz, J. E., Arrizubieta, J. I., Lamikiz, A., Ostolaza, M., 2022. Non-symmetrical design of coaxial nozzle for minimal gas consumption on L-DED process for Ti6Al4V reactive alloy. Journal of Manufacturing Processes 78, pp. 218–230.

Schmidt, M., Merklein, M., Bourell, D., Dimitrov, D., Hausotte, T., Wegener, K. et al., 2017. Laser based additive manufacturing in industry and academia. CIRP Annals 66 (2), pp. 561–583.

Sommerfeld, M., 1992. Modelling of Particle-Wall Collisions in Confined Gas-Particle Flows. Int. J. Multiphase Flow 18 (6), pp. 905–926.

Sommerfeld, M., Huber, N., 1999. Experimental analysis and modelling of particle-wall collisions. International Journal of Multiphase Flow 25 (6-7), pp. 1457–1489.

Tan, H., Zhang, C., Fan, W., Zhang, F., Lin, X., Chen, J., Huang, W., 2020. Dynamic evolution of powder stream convergence with powder feeding durations in direct energy deposition. International Journal of Machine Tools and Manufacture 157, p. 103606.